

Monte Carlo Analysis of Impulse Requirements for Injection Error Correction

Prabhakara P. Rao*

Martin Marietta Aerospace, Denver, Colo.

A comprehensive Monte Carlo statistical analysis is performed to investigate an optimum impulse requirement of a spacecraft in order to correct its injection errors. The covariance dispersion matrix is representative of both position and velocity errors about a nominal injection point of a geosynchronous mission. A mathematical model is used to obtain numerous simulations of perturbed orbits bounded by the injection error volume. An optimum two-impulse orbital transfer technique is applied to determine global minimum impulses to transfer from each of the perturbed orbits to a nominal or desired orbit. These global minimum impulses are then statistically treated to obtain probability histograms and to determine success probabilities and confidence limits associated with the impulses. A significant change in the distribution function is noticed when the desired orbit is different from the nominal orbit. A general discussion of the methodology used for the analysis is presented, along with some typical impulse requirements and their corresponding success probabilities.

Nomenclature

a, e, i, Ω, ω	= orbital elements (semimajor axis length, eccentricity, inclination, longitude of ascending node, argument of perigee)
N	= number of random perturbed orbits
P	= semilatus rectum
R, V	= radius and velocity vectors, respectively
S	= unbiased estimate of standard deviation
V_{T1}, V_{T2}	= transfer orbit velocity vectors at departure and arrival points
VX, VY, VZ	= velocity vector components
X, Y, Z	= radius vector components
ΔV	= total impulse
$\Delta V_1, \Delta V_2$	= impulses at departure and arrival points
$\frac{\Delta V}{N}$	= unbiased estimate of mean
α	= success probability
β	= confidence coefficient
ϵ	= confidence level ($= 1 - \beta$)
θ	= transfer angle
μ	= gravitational constant or population mean
μ_3, μ_4	= 3rd and 4th central moment
ν	= true anomaly
σ	= standard deviation

Subscripts

d, p	= desired and perturbed orbits, respectively
$1, 2$	= departure and arrival points, respectively

I. Introduction

IN order to attain an accurate orbit, a spacecraft should be capable of correcting its small injection dispersions. These dispersions may result from instrument and accumulated navigational errors of a launch vehicle during its flight time. To maximize weight allocations for scientific instruments, the least possible fuel the spacecraft should carry must be determined accurately.

Received July 22, 1977; presented as a paper at the AAS/AIAA Astrodynamics Conference, Jackson, Wyo., Sept. 7-9, 1977; revision received Nov. 28, 1977. Copyright © American Institute of Aeronautics and Astronautics, Inc., 1978. All rights reserved.

Index categories: Earth-Orbital Trajectories; Spacecraft Navigation, Guidance, and Flight-Path Control.

*Senior Engineer, Guidance and Navigation Unit. Member AIAA.

There are at least two basic approaches available to determine the fuel requirement for injection error correction. One method is to perform the worst-case analysis. The scheme is based on the selection of input parameters which require a maximum impulse for the correction. A major difficulty in applying this method to a complex orbital problem is to identify a proper combination of input parameters. Since these parameters are normally correlated, their extreme values do not produce a worst-case condition. Furthermore, the fuel requirement determined from this analysis may be unduly conservative.

An efficient and realistic approach is to calculate impulse requirements based on a Monte Carlo statistical analysis.¹ This technique is capable of accounting for nonlinearities in the mathematical model and non-Gaussian distribution of input or output variables. A large number of such variables makes the Monte Carlo method advantageous because of the prohibitive amount of analysis a parametric approach would require. In this scheme, the input variables are randomly selected from their probability distribution function. The computed impulses required for the correction are then analyzed statistically to yield their probability distribution. The purpose of this paper is to present the technical methodology involved in the application of the Monte Carlo method to determine the fuel requirement for the injection dispersion correction. It is demonstrated that this real-world simulation is a computationally feasible and efficient method to correct both position and velocity errors of a spacecraft. Furthermore, the impulse requirement to correct these errors is determined from a finite number of simulations by means of two separate confidence limit calculations for any specified success probability and confidence level.

II. Mathematical Analysis

A. Formulation

The Monte Carlo method of statistical analysis is used to investigate the theoretical fuel requirement to correct injection dispersions. The error sources² that affect both position and velocity errors at orbital insertion points are the uncertainties associated with accelerometers (bias, scale factor, misalignment), gyros (drift, anisoelectric, nonorthogonality), navigational errors, environmental effect, initial alignment errors, computer errors, and performance dispersions. Using a $1-\sigma$ deviation of these errors and a nominal flight trajectory, a covariance error matrix of state

variables can be determined by performing a preflight trajectory error analysis.

As a result of these errors, the spacecraft would achieve any one of a large number of possible orbits, which differs slightly from a nominal or desired orbit. Consequently, the problem of determining the spacecraft fuel requirement reduces to a statistical analysis of velocity increments required for optimum transfer from numerous perturbed orbits to a desired orbit.

A major consideration in the application of the Monte Carlo analysis is the simulation of perturbed orbits and determination of velocity increments for optimum orbital transfer. Each perturbed orbit is obtained by choosing random position and velocity components at the injection point from a statistical distribution of these variables. The average of the velocity increments for various perturbed orbits, along with variances and other measure of scatter, gives a statistically correct picture of the effect of injection uncertainties.

The Monte Carlo process requires generation of random state vectors from a 6×6 covariance matrix. Since the position and velocity errors are correlated, a transformation to a principal axis system provides the required error components in an uncorrelated space. The random error vector in the uncorrelated space is the product of a set of random numbers drawn from a normal distribution of mean 0 and variance 1 and the square root of eigenvalues of the covariance matrix. The random state vectors in the original coordinate system are obtained by transforming these error vectors from the principal axis system to the original coordinate frame. The orbital elements a_p , e_p , i_p , Ω_p , and ω_p , computed from these random state vectors, completely specify the perturbed orbit. The desired orbit is given by the orbital elements a_d , e_d , i_d , Ω_d , and ω_d . In the Monte Carlo scheme, a large number of random perturbed orbits are simulated, and impulse required for optimum transfer from each of these perturbed orbits to a desired orbit is considered.

B. Orbital Transfer

For the Monte Carlo analysis, a fast and efficient computational technique is required to determine optimal transfers from several perturbed orbits. Impulsive transfers simplify the computational equations and provide an insight into finite burn transfers. Optimum transfers between various types of orbits using one, two, and three impulses are discussed in a survey paper by Gobetz and Doll.³ An optimum single impulse, which can be used only to transfer between intersecting or tangent orbits, is equal or more than optimum two impulses. A three-impulse transfer between two widely separated noncoplanar orbits is optimum when the plane change is made during the intermediate impulse. In general, transfer between any two orbits can be achieved by a minimum of two impulses—one at a departure point and the other at an arrival point. Several investigators have studied the two-impulse transfer problem between two widely separated elliptical orbits^{4,6} with or without constraints on transfer angle and flight time. Since the presence of any such constraints increases the fuel requirement, no constraints are imposed in the present analysis.

The impulse required for a transfer with no constraints on its geometry depends on: 1) departure point true anomaly ν_p in the perturbed orbit, 2) arrival point true anomaly ν_d in the desired orbit, and 3) transfer orbit geometry. In previous studies, angles measured from a nodal line between two orbits have been used as independent variables. The choice of true anomalies has a definite advantage in the present problem, where transfers from a large number of perturbed orbits to a constant desired orbit is considered. Consequently, the same arrival point conditions can be used repeatedly without recomputations. The transfer orbit geometry is specified by using semilatus rectum as an independent variable, which simplifies the impulse function and avoids serious discon-

tinuities.⁴ In a simplified form, the impulse function can be written as $\Delta V = \Delta V(\nu_p, \nu_d, P)$. The objective of the optimal transfer is to determine ν_p , ν_d , and P for which total impulse ΔV is a minimum.

For any given departure and arrival points, represented by radius vectors $R_1(\nu_p)$ and $R_2(\nu_d)$, the required impulses are obtained from

$$\Delta V_1 = |V_{T1} - V_1| \quad \Delta V_2 = |V_{T2} - V_2| \quad \Delta V = \Delta V_1 + \Delta V_2 \quad (1)$$

where

$$V_{T1} = (R_2 - fR_1)/g \quad V_{T2} = (\dot{g}R_2 - R_1)/g \quad (2)$$

and

$$f = 1 - R_2(1 - \cos\theta)/P \quad g = 1 - R_1(1 - \cos\theta)/P$$

$$\dot{g} = (R_1 R_2 \sin\theta)/\sqrt{\mu P} \quad (3)$$

In the preceding equations, θ is the transfer angle between two radius vectors R_1 and R_2 , which may be less than 180 deg (short transfer) or more than 180 deg (long transfer). In this formulation, the transfer orbit plane is undefined for an exact 180 deg noncoplanar transfer, for which an additional parameter such as the transfer orbit inclination⁶ is available for optimization. Since 180 deg transfer is not an optimum transfer for noncoapsidal orbits, it is not considered in this analysis. To reduce computations, an intuitive judgment can be made on the type of transfer required for minimum impulse. Except for extreme cases where two orbits rotate in opposite directions, a forward motion should have a smaller impulse. Consequently, the transfer angle can be uniquely determined from the relation $\cos\theta = (R_1 \cdot R_2)/R_1 R_2$, where θ is greater than 180 deg when the dot product between the angular momentum vector of the perturbed orbit and normal vector to transfer orbit plane is negative.

Since the semilatus rectum P of the transfer orbit in Eq. (3) is an unknown quantity, an optimum value of P is determined iteratively by minimizing ΔV . The derivative of ΔV with respect to P required in the optimization process is obtained

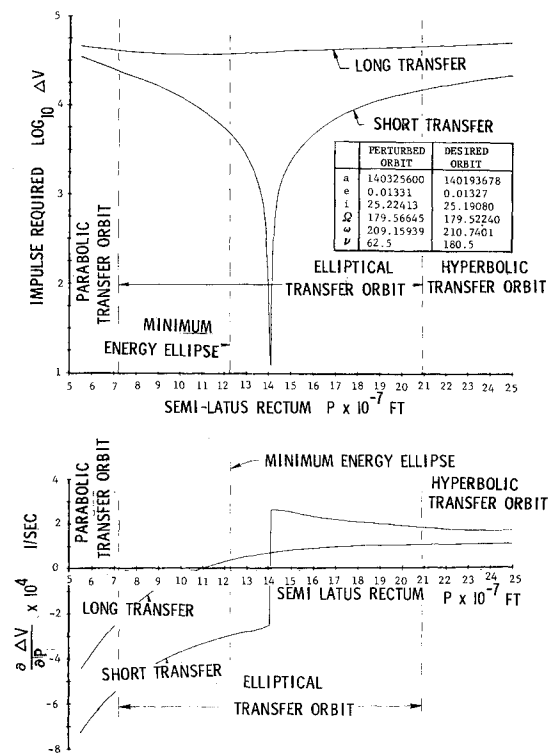


Fig. 1 Impulse function and its derivative.

from

$$\frac{\delta \Delta V}{\delta P} = \frac{1}{2gP} \left\{ \frac{(V_{T1} - V_I)}{\Delta V_I} \cdot [R_2 - (2-f)R_I] + \frac{(V_{T2} - V_2)}{\Delta V_2} \cdot [(2-g)R_2 - R_I] \right\} \quad (4)$$

At minimum impulse point, $\delta \Delta V / \delta P$ should be equal to zero or change its sign if discontinuity occurs. An impulse function, which can be obtained by equating $\delta \Delta V / \delta P$ to zero and certain squaring process, will be an octic equation. One positive root out of eight possible roots, which may be real or complex, of this octic equation determines the value of P for an absolute minimum total impulse. The squaring process adds four extraneous roots⁵ which do not correspond to the extrema of Eq. (4).

Instead of finding the roots of an octic equation and deciding which root corresponds to minimum ΔV , an effective numerical iterative technique is used. In general, the minimum impulse solution for a transfer between two elliptical orbits is an ellipse, and only one minimum occurs in that elliptical region. For some special cases, double minimum can occur and the minimum impulse solution can be hyperbola.⁵ A typical variation of ΔV and $\delta V / \delta P$ is shown in Fig. 1 for both short and long transfers covering all conics. Since $\delta \Delta V / \delta P$ changes discontinuously at a minimum impulse point, a *regula falsi* method is used to locate the minimum impulse point. Number of iterations and computational times are reduced by choosing the semilatus rectum of a minimum energy ellipse between R_I and R_2 as an initial guess. It should be noted that minimum energy ellipse is not a minimum impulse solution, except when two orbits are coapsidal.

C. Global Minimum Impulse

A global minimum impulse is an absolute minimum impulse required to transfer from a given perturbed orbit to a desired orbit. In the preceding section, the minimum impulse required to transfer between two points specified by v_p and v_d is presented. To determine the global minimum impulse, v_p and v_d are varied from 0-360 deg, and the minimum of all minimum impulses for transfers between all combinations of v_p and v_d is obtained. Figure 2 shows the locus of minimum transfer impulses for two different departure points of one particular perturbed orbit. In general, two local minimum points will be seen for every departure point—one corresponding to a short transfer and the other to a long transfer. The variation of minimum impulses required to

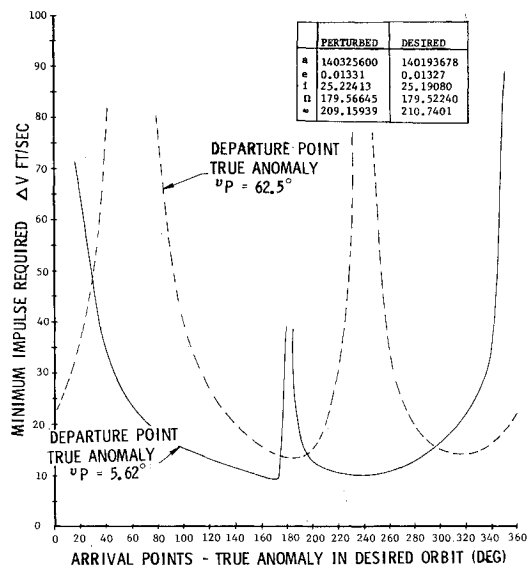


Fig. 2 Impulse required as a function of arrival point true anomaly.

transfer to the desired orbit as a function of departure true anomalies is depicted in Fig. 3, along with first and second impulses. One of the two local minima observed in this figure will be the required global minimum impulse. Although only two minimum points are noticed in this particular case, four minimum points normally occur in the $v_p - v_d$ space. To provide a better visualization, the minimum impulses at lattice points in the $v_p - v_d$ space are plotted (Fig. 4) in a three-dimensional view. The figure provides the extremum impulse regions, in addition to the impulse gradients, which will be useful to determine the computational step size.

Several different methods are available to determine the local minimum points in the $v_p - v_d$ space. Although a two-variable gradient method⁷ provides accurate results, it is computationally slow when several local minimum points exist in the search space. Also, an accuracy improvement of only 0.5% has been observed when compared to the present lattice point method with 10 deg step size. Since the departure and arrival points are normally in the vicinity of apogee and perigee, the accuracy of this lattice point scheme can be increased by using a nonuniform grid network with more points at apogee and perigee. Instead of these deterministic approaches, a statistical approach can also be used to determine the global minimum impulse. In this scheme, true anomalies v_p and v_d are selected randomly from a uniform or any specified distribution and optimum transfers are determined. A minimum impulse of all such optimal transfers will determine the global minimum impulse in the statistical sense.

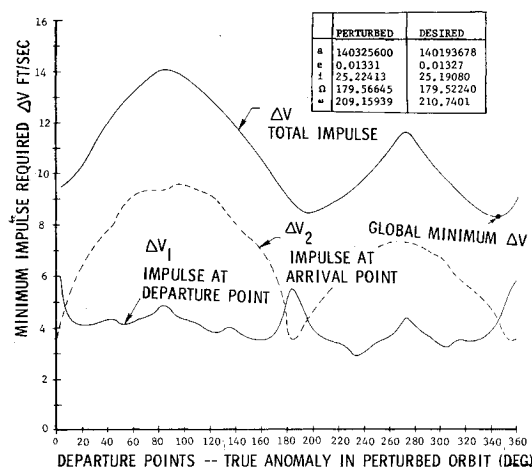


Fig. 3 Impulse required as a function of departure point true anomaly.

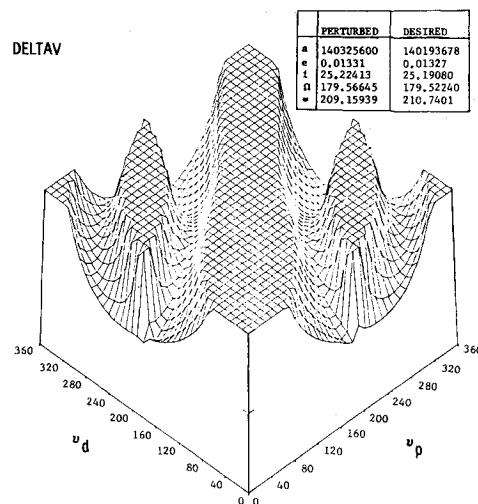


Fig. 4 Minimum impulse vs v_p and v_d .

D. Statistical Techniques

The two-impulse transfer technique provides global minimum impulses to transfer optimally from numerous perturbed orbits to a desired orbit. These impulses are treated statistically to provide an impulse requirement of a spacecraft. The fundamental statistical quantities of interest are the point estimate and confidence interval estimates. These statistical computations relate the calculated impulse requirement of a finite sample to its unknown value of an infinite population of the mathematical model.

The basic statistical outputs from the Monte Carlo Analysis are the frequency histogram and cumulative probability distribution of the optimum transfer impulses. From these results, a probabilistic statement can be made as

$$P_r(\Delta V \leq \Delta V_\alpha) = \alpha \quad (5)$$

where α is the probability that the required transfer impulse ΔV is less than ΔV_α . The objective of the statistical analysis is to estimate ΔV_α for any specified value of the success probability α . Although an exact determination of ΔV_α is not possible for a finite sample size, an estimate of this impulse can be made. For an infinitely large sample, the point estimate ΔV_α coincides with the true value ΔV_α . Since this point estimate exhibits a statistical variability, confidence limits may be calculated to provide a conservative estimate of this impulse.

For a given confidence coefficient β , the probability statement can be made for the confidence limits ΔV_{α_1} and ΔV_{α_2} as

$$P_r(\Delta V_{\alpha_1} \leq \Delta V_\alpha \leq \Delta V_{\alpha_2}) = \beta \quad (6)$$

where ΔV_{α_1} and ΔV_{α_2} are the lower and upper limits of ΔV_α determined from a finite sample, and β is the probability that ΔV_α will be within ΔV_{α_1} and ΔV_{α_2} . The point estimate ΔV_α and its confidence limits ΔV_{α_1} and ΔV_{α_2} can be calculated either by assuming no knowledge of the distribution function (distribution-free or nonparametric estimation) or by determining its theoretical distribution function (parametric estimation).

In the nonparametric method, the samples of N global minimum impulses are arranged in increasing order of magnitude. The point estimate ΔV_α is that impulse which is not exceeded by αN times. The nonparametric confidence limits are obtained from the binomial for quartiles. If the sample size is large ($N > 30$), the binomial frequency distribution can be approximated by a normal distribution with mean $N\alpha$ and variance $N\alpha(1-\alpha)$. To find the confidence interval $\alpha_1 < \alpha < \alpha_2$ with confidence level $\epsilon (= 1-\beta)$, α_i ($i=1,2$) are obtained by solving quadratic equation⁸

$$\alpha_i^2(1 + K_\epsilon^2/N) - \alpha_i(2\alpha + K_\epsilon^2/N) + \alpha^2 = 0 \quad (7)$$

where K_ϵ is obtained from

$$\epsilon/2 = (1/\sqrt{2\pi}) \int_{K_\epsilon}^{\infty} e^{-t^2/2} dt \quad (8)$$

The normal distribution approximation also enables us to determine the number of samples required so that 100 α % of

Table 2 Dispersions in orbital elements

Orbital element	Nominal value	99.7% probability limit
a , ft	140193678	140407102
e	0.01327	0.01384
i , deg	25.1908	25.2753
Ω , deg	179.5224	179.6773
ω , deg	210.7401	216.5089

the population is less than the largest value of the impulse in the sample with 100 β % confidence. Equating α_2 to unity and solving for N in Eq. (7), the required sample size is obtained approximately by $N = \alpha K_\epsilon^2 / (1-\alpha)$.

Another approach to determine the confidence interval is to use the Kolmogorov-Smirnov test, which provides a maximum bandwidth between the observed and theoretical cumulative probability distributions. The maximum deviation D is given by $D = \max |F(\Delta V) - S_N(\Delta V)|$, where $F(\Delta V)$ and $S_N(\Delta V)$ are the population and sample cumulative probability that impulses are less or equal to any ΔV value. The critical values of D are available in many statistical texts⁹ for any given sample size N and confidence coefficient β .

The parametric estimation is based on the ability to predict the population distribution function from a sample distribution. This hypothesis can be investigated by means of statistical goodness-of-fit tests, such as the chi-square test⁸ and the Kolmogorov-Smirnov test.⁹ If the impulse distribution is Gaussian, which is normally the case when the nominal and desired orbits are different, simplified expressions can be obtained for the point estimate and confidence limits. For a normal distribution with mean μ and standard deviation σ , the 100 α % probability impulse limit is given by

$$\Delta V_\alpha = \mu + K_\alpha \sigma \quad (9)$$

where K_α is obtained from

$$\alpha = (1/\sqrt{2\pi}) \int_{-\infty}^{K_\alpha} e^{-t^2/2} dt \quad (10)$$

If $\bar{\Delta V}$ and S are the unbiased sample estimates of mean and standard deviation, respectively, the point estimate of this impulse limit will be

$$\hat{\Delta V}_\alpha = \bar{\Delta V} + K_\alpha S \quad (11)$$

The confidence limits ΔV_{α_1} and ΔV_{α_2} corresponding to Eq. (6) can be written in the form

$$\Delta V_{\alpha_i} = \bar{\Delta V} + (K_\alpha + K_i) S \quad i=1,2 \quad (12)$$

where K_i ($i=1,2$) are obtained for large sample size ($N > 50$) by solving the quadratic equation

$$K_i^2(1 - K_\epsilon^2/2N) - K_\alpha K_i^2 K_i / N - K_\epsilon^2(2 + K_\alpha^2)/2N = 0 \quad (13)$$

where K_α and K_ϵ are determined from Eqs. (10) and (8), respectively. Note that K_i depends on the probability limit α , confidence level ϵ , and sample size N . As the sample size

Table 1 Injection error covariance matrix

	X	Y	Z	VX	VY	VZ
X	2.10085E10					
Y	-6.37475E9	2.41587E9				
Z	4.06302E9	-5.71464E9	2.18286E9			
VX	1.88405E6	-5.57217E5	3.75600E5	1.75628E2		
VY	6.37269E5	-1.86806E5	1.19246E5	6.54303E1	3.31825E1	
VZ	-2.37497E5	8.24137E4	-6.23301E4	-9.51418E0	1.21505E1	3.61232E1

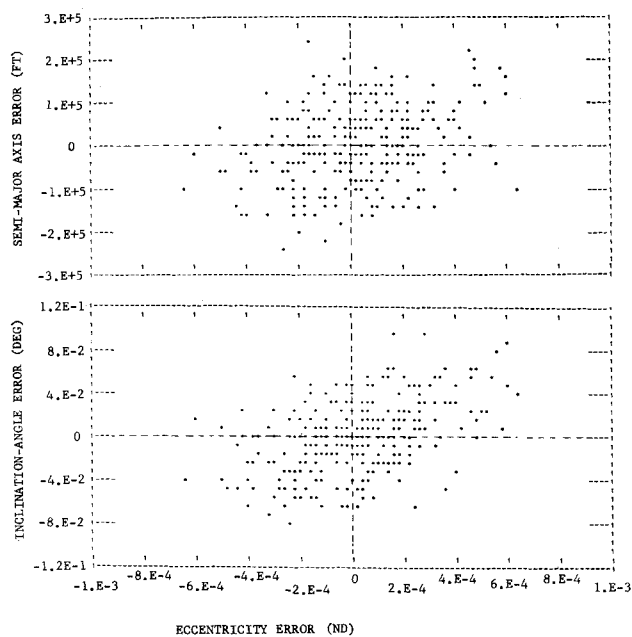


Fig. 5 Scattergram of Semimajor axis length and inclination.

increases, the confidence interval decreases for the same confidence level. If the impulse distribution can be assumed with reasonable certainty to be normal, then the parametric confidence limits may be used to obtain the impulse requirement value at a higher probability level.

III. Numerical Results

In order to validate the analysis method, computer runs were made using orbit insertion errors of a geosynchronous mission. The covariance matrix, which represents both position and velocity errors, results from the propagation of instrument errors of a carouseling IMU (inertial measurement unit) along a typical Titan IIIC flight trajectory from lift-off up to the final orbit injection. Since the covariance matrix is symmetrical, only the lower half of the input data in the ECI (Earth centered inertial) frame is shown in Table 1, in which diagonal terms are the variances of position (ft²) and velocity errors (ft²/s²), and off-diagonal terms represent their correlation.

In the present analysis, 300 random perturbed orbits are generated using 1800 random numbers drawn from a Gaussian distribution. To insure that these numbers truly represent a normal distribution, their mean and variances are determined, which are found to be 0 and 1 within a stringent tolerance. Although several variance-reducing techniques¹⁰ are available to reduce statistical errors without increasing the number of simulations required, none of them are found to be suitable. However, an initial seed in the generation of random numbers is selected in order that the running mean and standard deviation converge faster. This will, in effect, reduce the number of samples required to provide a well-defined distribution function.

The Monte Carlo scheme enables the determination of dispersions in the orbital elements. The nominal orbital elements and their 99.7% probability limit obtained using the injection covariance error matrix are presented in Table 2. The injection point true anomaly is 5.62 deg.

A scattergram of errors in the semimajor axis length and inclination with respect to the eccentricity error, presented in Fig. 5, depicts a positive correlation. The type of correlation depends on the nominal injection orbit and injection point location. Due to the presence of this correlation, a complete covariance matrix should be considered for the fuel requirement analysis, instead of separately considering the individual errors in the orbital elements.¹¹

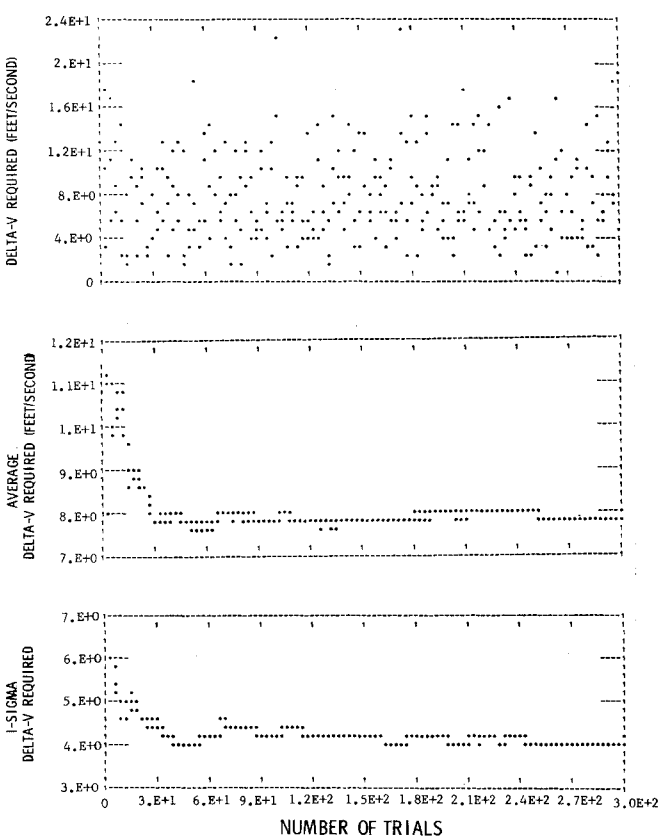


Fig. 6 Minimum impulses, mean and 1-σ variations.

The global minimum impulses for transfers from 300 perturbed orbits to a nominal orbit are shown in Fig. 6. The running mean and 1-σ value approach constant values, indicating that 300 random orbits are sufficient to predict the behavior of ΔV distribution function. Furthermore, a 20- × 20-deg grid size in the $v_p - v_d$ search space provides a fairly accurate ΔV distribution, as illustrated in Table 3, and reduces computation time by nearly 25%. Computer time required for the Monte Carlo simulation of 300 random perturbed orbits and 20 deg grid search for optimization is approximately 3 min on a CDC 6500 computer.

Table 3 Effect of grid size on ΔV distribution function

Properties of ΔV distribution function	20- × 20-deg grid size	10- × 10-deg grid size
Mean	7.91234	7.86797
Standard deviation (σ)	4.10402	4.09076
Variance (σ ²)	16.84300	16.73430
Skewness (μ ₃ /σ ³)	0.89214	0.90529
Kurtosis (μ ₄ /σ ⁴)	3.82627	3.87342

Table 4 Comparison with Gaussian distribution

Properties	ΔV distribution	Gaussian distribution
Mean	208.92876	208.92876
Standard deviation	6.25901	6.25901
Variance	39.17515	39.17515
Skewness	-0.02486	0.0
Kurtosis	3.09607	3.0
95% probability limit	219.41	221.21
99.7% probability limit	225.73	227.71

DELTA-V-REQUIRED STATISTICS

CLASS BOUNDARIES	FREQUENCY	HISTOGRAM OF FREQUENCY
7.36774E-01		0
1.85835E+00	6	21.5
2.97993E+00	17	43
4.10151E+00	34	
5.22309E+00	26	
6.34467E+00	43	
7.46625E+00	33	
8.58783E+00	26	
9.70941E+00	29	
1.08310E+01	20	
1.19526E+01	15	
1.30741E+01	15	
1.41957E+01	11	
1.53173E+01	12	
1.64389E+01	2	
1.75605E+01	4	
1.86820E+01	3	
1.98036E+01	1	
2.09252E+01	0	
2.20468E+01	0	
2.31684E+01	3	

CLASS BOUNDARIES	CUMULATIVE FREQUENCY	CUMULATIVE FREQUENCY PLOT
7.36774E-01		0
1.85835E+00	.02000	0.5
2.97993E+00	.07667	1
4.10151E+00	.19000	
5.22309E+00	.27667	
6.34467E+00	.42000	
7.46625E+00	.53000	
8.58783E+00	.61667	
9.70941E+00	.71333	
1.08310E+01	.78000	
1.19526E+01	.83000	
1.30741E+01	.88000	
1.41957E+01	.91667	
1.53173E+01	.95667	
1.64389E+01	.96333	
1.75605E+01	.97667	
1.86820E+01	.98667	
1.98036E+01	.99000	
2.09252E+01	.99000	
2.20468E+01	.99000	
2.31684E+01	1.00000	

MEAN = 7.9123 STANDARD DEVIATION = 4.104

Fig. 7 Histogram and cumulative probability diagram when nominal and desired orbits are the same.

The frequency histogram and cumulative probability diagram, presented in Fig. 7, show that an asymmetric distribution will be obtained when the desired orbit is a nominal orbit. For this case, the nominal transfer ΔV is zero, whereas the impulses required for all perturbed orbits are greater than zero. Since the mode of the distribution is to the left of its mean value, it is positively skewed and the Pearson's measure of skewness, (mean-mode)/ σ , is found to be about 0.52. This frequency distribution closely resembles a chi-square distribution with mean equal to 8.

A significant change in the shape of frequency distribution will be noticed if the desired orbit is different from a nominal orbit. The frequency histogram and cumulative probability diagram for a case in which the desired orbit inclination is 24 deg instead of a nominal 25.1908 deg is shown in Fig. 8. The nominal impulse required for the transfer is 205.90216 ft/s. Since the perturbed orbit transfer impulses can occur on either side of this nominal value, the frequency distribution approaches a Gaussian distribution, which has been verified by a chi-square goodness-of-fit test. The properties of ΔV and Gaussian distributions are shown in Table 4.

The deviations in skewness and kurtosis (a measure of flatness) from their corresponding Gaussian distribution values are due to random variations in the selection of the sample. Significance tests on these parameters¹² showed that they are well within the significance limit for 300 samples with a significance level as low as 1%. Compared to a normal distribution, the actual sample ΔV distribution is leptokurtic.

In Fig. 9, the 99% confidence limits about the cumulative probability estimate are shown for two cases: 1) nominal and desired orbits are the same, and 2) desired orbit inclination is 24 deg, instead of a nominal value of 25.1908 deg. The largest value of the impulse observed in the actual 300 samples corresponds to a nonparametric probability level of 99% with 90% confidence or a probability level of 98.6% with 95%

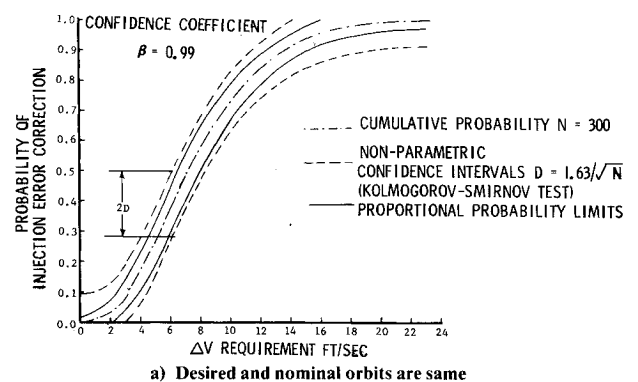
DELTA-V-REQUIRED STATISTICS

CLASS BOUNDARIES	FREQUENCY	HISTOGRAM OF FREQUENCY
1.87712E+02		0
1.89712E+02	1	24.0
1.91713E+02	0	48
1.93714E+02	0	
1.95714E+02	2	
1.97715E+02	10	
1.99716E+02	13	
2.01716E+02	15	
2.03717E+02	16	
2.05718E+02	31	
2.07718E+02	30	
2.09719E+02	48	
2.11720E+02	36	
2.13720E+02	34	
2.15721E+02	22	
2.17722E+02	16	
2.19722E+02	13	
2.21723E+02	9	
2.23724E+02	0	
2.25724E+02	2	
2.27725E+02	2	

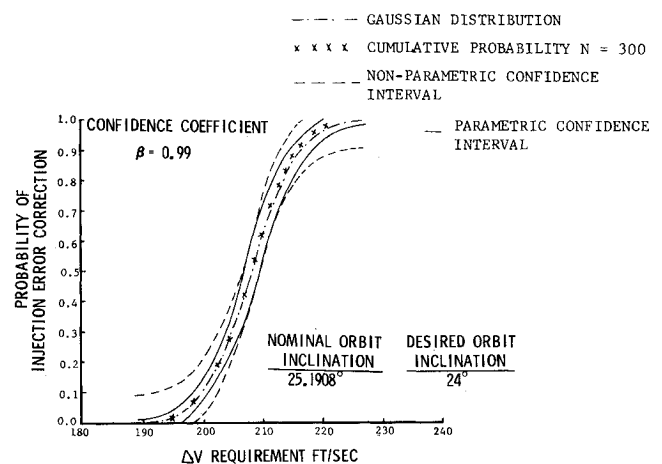
CLASS BOUNDARIES	CUMULATIVE FREQUENCY	CUMULATIVE FREQUENCY PLOT
1.87712E+02		0
1.89712E+02	.00333	0.5
1.91713E+02	.00333	1
1.93714E+02	.00333	
1.95714E+02	.01000	
1.97715E+02	.04333	
1.99716E+02	.08667	
2.01716E+02	.13667	
2.03717E+02	.19000	
2.05718E+02	.29333	
2.07718E+02	.39333	
2.09719E+02	.55333	
2.11720E+02	.67333	
2.13720E+02	.78667	
2.15721E+02	.86000	
2.17722E+02	.91333	
2.19722E+02	.95667	
2.21723E+02	.98667	
2.23724E+02	.98667	
2.25724E+02	.99333	
2.27725E+02	1.00000	

MEAN = 208.9287 STANDARD DEVIATION = 6.259

Fig. 8 Histogram and cumulative probability diagram when nominal and desired orbits are different.



a) Desired and nominal orbits are same



b) Desired and nominal orbits are different

Fig. 9 Confidence limits.

confidence. The confidence interval is a function of probability level, confidence coefficient, and sample size. The interval decreases with increase of sample size, whereas it increases with confidence coefficient. Both parametric and nonparametric methods provide approximately the same upper and lower impulse requirements in the 50% probability region. However, the parametric method estimates a smaller interval in low and high probability regions, due to its ability to accurately define the outer region of the ΔV distribution.

IV. Conclusion

A feasibility study has been performed to determine the fuel requirement of a geosynchronous satellite to correct its injection errors using the Monte Carlo statistical analysis. The method is capable of correcting both position and velocity errors by finding optimum transfers to a nominal or desired orbit. Both nonparametric and parametric confidence limits efficiently and conservatively determine the impulse requirements at any probability level from a finite sample. A significant change in the impulse distribution is noticed when the nominal and desired orbits are different. For a comprehensive analysis of a spacecraft fuel requirement, this Monte Carlo scheme is found to be appropriate and very useful.

Acknowledgment

The author would like to express his thanks to T.L. Roberts for the support during the investigation and L.E. Best for incorporating the histogram plotting capabilities to the program.

References

- ¹Hammersley, J.M. and Handscomb, D.C., *Monte Carlo Methods*, Methuen, London, 1964.
- ²Fernandez, M. and MaComber, C.R., *Inertial Guidance Engineering*, Prentice-Hall Inc., Englewood Cliffs, N.J., 1962.
- ³Gobetz, F.W. and Doll, J.R., "A Survey of Impulsive Trajectories," *AIAA Journal*, Vol. 7, May 1969, pp. 801-834.
- ⁴McCue, G.A., "Optimum Two-Impulse Orbital Transfer and Rendezvous between Inclined Elliptical Orbits," *AIAA Journal*, Vol. 1, Aug. 1963, pp. 1865-1872.
- ⁵Lee, G., "An Analysis of Two-Impulse Orbital Transfer," *AIAA Journal*, Vol. 2, Oct. 1964, pp. 1767-1773.
- ⁶Sun, F.T., "Analytic Solution for Optimal Two-Impulse 180° Transfer between Noncoplanar Orbits and the Optimal Orientation of the Transfer Plane," *AIAA Journal*, Vol. 7, Oct. 1969, pp. 1898-1904.
- ⁷McCue, G.A. and Bender, D.F., "Numerical Investigation of Minimum Impulse Orbital Transfer," *AIAA Journal*, Vol. 3, Dec. 1965, pp. 2328-2334.
- ⁸Burlington, R.S. and May, D.C., *Handbook of Probability and Statistics with Tables*, Handbook Publishers, Inc., Ohio, 1958.
- ⁹Siegel, S., *Nonparametric Statistics for the Behavioral Sciences*, McGraw-Hill Book Co., New York, 1956.
- ¹⁰Kahn, H., "Use of Different Monte Carlo Sampling Techniques," *Symposium on Monte Carlo Methods*, Wiley, New York, 1956, pp. 146-190.
- ¹¹Edelbaum, T.N., "Propulsion Requirements for Controllable Satellites," *ARS Journal*, Vol. 31, Aug. 1961, pp. 1079-1089.
- ¹²Croxtan, F.E. and Cowden, D.J., *Applied General Statistics*, Prentice-Hall, Inc., Englewood Cliffs, N.J., 1955.

From the AIAA Progress in Astronautics and Aeronautics Series...

EXPERIMENTAL DIAGNOSTICS IN GAS PHASE COMBUSTION SYSTEMS—v. 53

Editor: Ben T. Zinn; Associate Editors: Craig T. Bowman,
Daniel L. Hartley, Edward W. Price, and James F. Skifstad

Our scientific understanding of combustion systems has progressed in the past only as rapidly as penetrating experimental techniques were discovered to clarify the details of the elemental processes of such systems. Prior to 1950, existing understanding about the nature of flame and combustion systems centered in the field of chemical kinetics and thermodynamics. This situation is not surprising since the relatively advanced states of these areas could be directly related to earlier developments by chemists in experimental chemical kinetics. However, modern problems in combustion are not simple ones, and they involve much more than chemistry. The important problems of today often involve nonsteady phenomena, diffusional processes among initially unmixed reactants, and heterogeneous solid-liquid-gas reactions. To clarify the innermost details of such complex systems required the development of new experimental tools. Advances in the development of novel methods have been made steadily during the twenty-five years since 1950, based in large measure on fortuitous advances in the physical sciences occurring at the same time. The diagnostic methods described in this volume—and the methods to be presented in a second volume on combustion experimentation now in preparation—were largely undeveloped a decade ago. These powerful methods make possible a far deeper understanding of the complex processes of combustion than we had thought possible only a short time ago. This book has been planned as a means of disseminating to a wide audience of research and development engineers the techniques that had heretofore been known mainly to specialists.

671 pp., 6x9, illus., \$20.00 Member \$37.00 List

TO ORDER WRITE: Publications Dept., AIAA, 1290 Avenue of the Americas, New York, N.Y. 10019